Electronic Supplementary Material (ESI) for Materials Chemistry Frontiers.

Supporting information

One-step Simultaneously Regulating Planarization and Donor Rotation to Enhance the multi-modal imaging Guiding Therapy

Yize Zhang†, Junjun Wang†, Shen Wang, Xiaojiao Zhu, Zhipeng Yu, Zhichao Wu, Jianhua Yu, and Hongping Zhou*

School of Chemistry and Chemical Engineering, Institute of Physical Science and Information Technology, Anhui Province Key Laboratory of Functional Inorganic Materials Chemistry of Anhui Province, Anhui Province Key Laboratory of Chemistry for Inorganic/Organic Hybrid Functionalized Materials, Anhui University, Hefei 230601, P. R. China

†These authors contributed equally to this work

*Prof. Hongping Zhou, E-mail: zhpzhp@263.net

Table of Contents

Materials.

All general chemicals for organic synthesis and fluorescence detection were purchased from commercial sources (Aladdin, Macklin, Sigma-Aldrich, Bioquest, and Thermo), including 2, 7-dichloro fluorescein diacetate (H_2DCF-DA), 9, 10-anthracenediylbis (methylene)-dimalonic acid (ABDA), aminophenyl fluorescein (APF), JC-10, 5, 5-Dimethyl-1-pyrroline N-oxide (DMPO), dulbecco's modified eagle medium (DMEM), and 3-(4, 5-dimethylthiazol-2-yl)-2, 5-diphenyltetrazolium bromide (MTT), Mito-Tracker Green, Lyso-Tracker Green, Annexin V-FITC/PI and Calcein-AM/PI Double Stain Kit was obtained from commercial sources (Aladdin, Macklin, Sigma Aldrich, Bioquest and Thermo). Human hepatocellular 4/25 carcinoma cell (HepG2), Mouse hepatoma cell (H22 cells) and Mouse alveolar macrophages (MH-S cells) were purchased from BeNa culture collection. BALA/c nude mice were given by Shanghai sipul-bikai laboratory animal *Co., Ltd.* All reagents and solvents used in syntheses were commercially available at analytical grade and were used without further purification.

Characterization.

^{1}H and ^{13}C-NMR were measured on Bruker AVANCE instruments using the dimethyl sulfoxide-d_6 (DMSO-d_6) as solvents (400 MHz for ^{1}H NMR and 100 MHz for ^{13}C NMR), and tetramethylsilane (TMS; δ = 0 ppm). Mass spectra were performed on a mass spectrometer with LTQ Orbitrap XL. The morphologies of prepared photosensitizers were investigated by JEM-2100 High Resolution-Transmission Electronic Microscope (TEM). EPR spectrum was examined on a Bruker Nano x-band spectrometer. Cell imaging was taken on ZEISS710 and Olympus FV 1200 MPE-share confocal laser scanning microscope (CLSM). The X-ray diffraction measurements were performed on a CCD area detector using graphite monochromated MoKα radiation (λ = 0.71069 Å) at 298(2) K.

***In vitro* $^1O_2$ detection.**

9, 10-anthracenedipropanoic acid (ABDA) was employed as the $^1O_2$ indicator. In this experiment, 3 mL PS solution (10 μM) was added into 5 mL centrifuge tubes and 13 μL of ABDA stock solution (7.5 mM) was added in dark conditions. The absorbance of ABDA at 378 nm was recorded at various times (every 10 seconds) to obtain the decomposition rate of ABDA in the photosensitizing process.

***In vitro* ROS detection.**

The generation of ROS was detected by using DCFH-DA as the indicator. DCFH-DA stock solution (2 mM) was freshly prepared. DCFH-DA solution (100 μL, 2 mM) was activated by NaOH solution (0.8 mL, 0.01 M) for 30 min in dark. And then, the above solution was added to 4.1 mL PBS. The AIE-PSs (1 mM, 50 μL) were added to the centrifuge tubes. Then they are irradiated by white light at different times. The emission of DCFH-DA at 530 nm was recorded at various times (every second) to obtain the decomposition rate of the photosensitizing process.

Detecting $^{\bullet}OH$ and $^1O_2$ generation *via* electron paramagnetic resonance (EPR) assay.

The EPR assay was carried out with a Bruker Nano x-band spectrometer using 5, 5-dimethyl-1-pyrroline N-oxide (DMPO) as a spin-trap agent. **TPA-OS**, **TPA-OS**, and **TPA-2T-OS** were dissolved in water at a dilution of 10 mM, and then 25 mM DMPO was added into the water without and with irradiation (laser; 1 W/cm^2) for 5 minutes respectively. Finally, the EPR signal was recorded at room temperature. The Nano X-band system from Bruker (Germany) was used to record the electron spin resonance (ESR) spectra to assess $^{\bullet}OH$ and $^1O_2$ production by the irradiated sample. Room-temperature ESR measurement was performed at the School of Chemistry and Chemical Engineering, Anhui University.

Photothermal properties tests.

The solution of **TPA-OS**, **TPA-T-OS**, and **TPA-2T-OS** (100 μM) was irradiated by a 720 nm laser at power densities of 1 W cm^{-2}. The temperature changes were monitored by FLIR E8-XT camera. The solutions of **TPA-OS**, **TPA-T-OS**, and **TPA-2T-OS** (100 μM) were exposed to 720 nm laser irradiation at 1 W cm^{-2} for 4 minutes when their temperature reached a plateau. At this time point, the laser was shut off. Then the solution was cooled down to room temperature. The temperature of the solution was recorded at an interval of 10 s during this process. The photothermal conversion efficiency was determined according to Equation a), and the other parameters in the equation a) were calculated from equations b), c), and d).

$$\eta = \frac{hS(T_{max} - T_{surr}) - Q_{Dis}}{I(1 - 10^{-A_{660}})} \quad \text{a)}$$

$$\tau_s = \frac{\sum_i m_i C_{p,i}}{hS} \quad \text{b)}$$

$$t = \tau_s(-\ln\theta) \quad \text{c)}$$

$$\theta = \frac{T - T_{surr}}{T_{max} - T_{surr}} \quad \text{d)}$$

In equation a), $\boldsymbol{\eta}$ is the photothermal conversion efficiency, $\boldsymbol{h}$ is the heat transfer coefficient; $\boldsymbol{S}$ is the surface area of the container. $\boldsymbol{Q_{Dis}}$ represents heat dissipated from the laser mediated by the solvent and container. $\boldsymbol{I}$ is the laser power and A_{660} is the absorbance of the sample at 720 nm. In equation b), $\boldsymbol{m}$ is the mass of the solution containing the photoactive material, C is the specific heat capacity of the solution (C_{water} = 4.2 J g^{-1}). In equation c), $\boldsymbol{\tau_s}$ is the associated time constant. In equation d), $\boldsymbol{\theta}$ is a dimensionless parameter, known as the driving force temperature. $\boldsymbol{T_{max}}$ and $\boldsymbol{T_{Surr}}$ are the maximum steady-state temperature and the environmental temperature, respectively.

Cell culture and imaging.

Cells were cultured in cell culture dishes with Dulbecco's modified eagle medium (DMEM) medium containing 10 % fetal bovine serum (FBS) and incubated at 37 °C in an air atmosphere (21% and 5% O_2). In fluorescence imaging experiments, the cells were planted into glass-bottom

dishes (15 × 15 mm) for cell apoptosis experiments (Annexin V-FITC/PI). After 10 μM of **TPA-OS**, **TPA-T-OS**, and **TPA-2T-OS** were added and cultivated for 30 min at 37 °C, the dishes were washed with PBS (pH 7.2) three times. The cell images were acquired via ZEISS710 and Olympus FV 1200 MPE-share confocal laser scanning microscope with a 10× or 60 × objective lens.

Live/Dead cell stain experiment for evaluating the efficiency of photodynamic therapy.

HepG2 cells were pre-cultured into 15 mm ×15 mm confocal dishes and incubated for 24 h. After incubated with 10 μM PSs for 30 min in a 21% and 5% O_2 atmosphere at 37℃, the cells were further stained by 10 μM photosensitizers and Annexin V-FITC for 30 min. Usually, Annexin V-FITC-PI staining dead cells would exhibit red fluorescence in the nucleus and green fluorescence in the cell membrane during cell apoptosis. Green channel Annexin V-FITC (λex = 495 nm, λem = 530 nm) and red channel PI (λex = 488 nm, λem = 630 nm)

Biocompatibility measurement

Dark cytotoxicity evaluation.

HepG2 cells were seeded into 96-well plates at a density of 10^4 cells/mL. After 12 h incubation, different concentrations (0, 2.5, 5, 10, 15, 20 μM) of **TPA-OS**, **TPA-T-OS** and **TPA-2T-OS** were added and incubated for another 24 h at 37 ^{0}C, 5% CO_2. MTT with 10 μL (5 mg/mL in PBS) was added for another 4 h. 150 μL DMSO was then added into each well with purple formazan crystals. The absorbance of the sample in each well was recorded at 490 nm by a multi-detection microplate Reader.

Light cytotoxicity evaluation.

HepG2 cells were seeded into 96-well plates at a density of 10^4 cells/mL. After 12 h incubation, different concentrations (0, 2.5, 5, 10, 15, 20 μM) of **TPA-OS**, **TPA-T-OS** and **TPA-2T-OS** were added and incubated for another 24 h at 37 ^{0}C, 5% CO_2. Subsequently, the wells were exposed to white light for 10 min. Finally, the same treatments were carried out following the above-mentioned process. All tumor-bearing mice were randomly divided into five groups: control (light -), control (light +), **TPA-2T-OS** (light -), **TPA-2T-OS** (light +) groups.

***In vitro* and *in vivo* PAI.**

In vitro and *in vivo* PA images were obtained by using the MSOT imaging technique: PBS solution of **TPA-2T-OS** at different concentrations was used for PA signal detection. To perform *in vivo* PAI, H22 tumor-bearing mice were injected with **TPA-2T-OS**. Then, the mice were sedated with an anesthetic gas, which was 5% isoflurane mixed with air. The tumor sites at different time points (0, 1, 2, 3, 4, 5, 6, 7, and 8 h) were scanned *via* the MSOT in the Vision 128 system (iThera Medical GmbH, Munich, Germany).

Photodynamic therapy *in vivo*.

The suspension of cells (10^8 cells/mL, H22 cells) was obtained and then subcutaneously injected into the female BALB/c nude mice (28-35 days). Then the H22-bearing mice were kept in SPF condition, protected from light, and fed and watered freely. After 3-days inoculation, the tumor size was appropriate and the tumor nude mice were split into four groups (3 mice each), treated as below: a) control, b) control + light, c) **TPA-2T-OS** (10^{-4} M, 100 μL), (d) **TPA-2T-OS** (10^{-4} M, 100 μL) + light. Notably, only a single-dose injection was employed during *in vivo* treatment process. Additionally, the volume of the tumor was calculated by the formula: (length × width^2) /2.

Synthesis

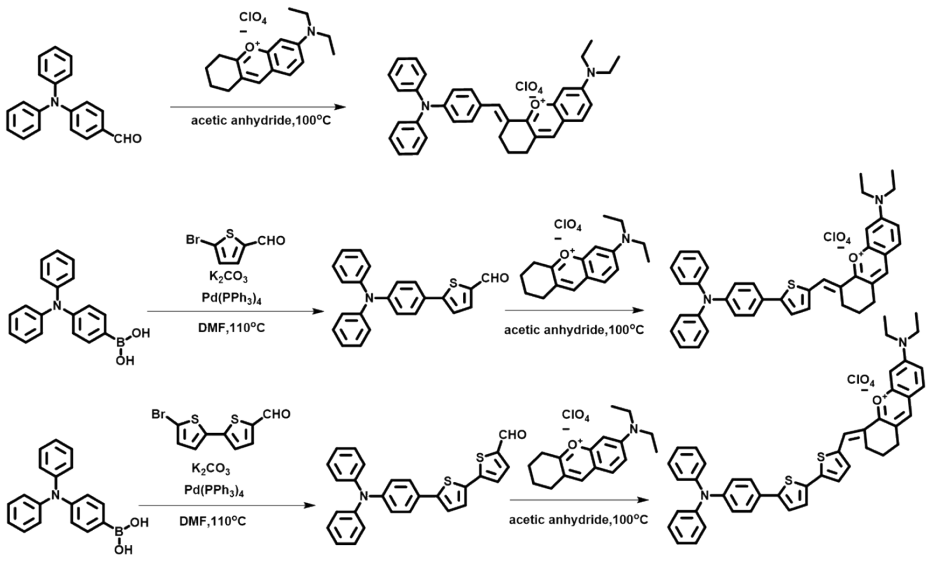

Scheme S1. The synthetic routes for compounds **TPA-OS**, **TPA-T-OS**, and **TPA-2T-OS**.

Synthesis of TPA, TPA-T, TPA-2T.

The starting materials TPA, TPA-T, and TPA-2T were either commercially available or prepared through literature methods. [S1]

Synthesis of TPA-OS.

A mixture of 4-(diphenylamino) benzaldehyde (1.00 g, 3.66 mmol) and 6-(diethylamino)-1, 2, 3, 4-tetrahydroxanthylium (1.30 g, 3.66 mmol) in acetic anhydride (20.0 mL) were refluxed for 6 h. Then, the cooled mixture was concentrated in vacuum. The crude product was purified by column chromatography with dichloromethane (DCM) and methanol (v/v = 10:1) as an eluent. Finally, **TPA-OS** (1.96 g, yield: 87.7 %) was obtained as blue powders. ^{1}H NMR (400 MHz, DMSO-d_6) δ: 8.4273 (s , 1H) ,7.9729 (s , 1H) , 7.8420 - 7.8185 (*d* , *J* = 9.4 Hz, 1H), 7.5614 - 7.5392 (*d*, *J* = 8.88 Hz, 2H), 7.3997 - 7.3454 (m, 5H), 7.2188 - 7.1116 (m, 7H), 6.9156 - 6.8936 (*d* , *J* = 8.8 Hz, 2H), 3.6793 - 3.6272 (m, 4H), 3.3029 (s, 1H), 2.8919 - 2.8668 (t, *J* = 5.02 Hz, 2H), 2.8260 - 2.7271 (t, *J* = 5.78 Hz, 2H), 1.8238 - 1.7960 (t, *J* = 4 Hz, 2H), 1.2258 - 1.1897 (t, *J* = 7.22 Hz, 6H). ^{13}C NMR

(100 MHz, DMSO-d_6): δ (*ppm*) 163.3469, 158.8692, 155.0570, 149.5697, 148.4119, 146.4068, 137.1074, 133.4817, 132.3119, 130.4539, 128.2815, 125.4788, 123.6768, 120.066, 118.8424, 46.0110, 41.2881, 34.7371, 22.9949, 13.0912. HR-MS (ESI): $[M]^+$ calcd for $C_{36}H_{35}N_2O^+$ 511.2744, found, 511.2724.

Synthesis of TPA-T-OS.

A mixture of TPA-T (0.50 g, 1.40 mmol) and 6-(diethylamino)-1, 2, 3, 4-tetrahydroxanthylium (0.60 g, 1.68 mmol) in acetic anhydride (15.0 mL) were refluxed for 5 h. Then, the cooled mixture was concentrated in vacuum. The crude product was purified by column chromatography with DCM and methanol (v/v = 10:1) as an eluent. Finally, **TPA-T-OS** (0.62 g, yield: 64.1 %) was obtained as blue powders. ^{1}H NMR (400 MHz, DMSO-d_6) δ: 8.4445 (s, 1H), 8.2820 (s, 1H), 7.8562 - 7.8362 (d, J = 9.44 Hz, 1H), 7.7005 - 7.6219 (m , 4H), 7.4131 - 7.3835 (m, 1H), 7.3504 - 7.3108 (t, J = 7.92 Hz, 4H), 7.2096 - 7.2023 (*d*, J = 2.92 Hz, 1H), 7.1178 - 7.546 (m, 6H), 6.9550 - 6.9379 (*d*, J = 6.84 Hz, 2H), 3.6963 - 3.6412 (m, 4H), 2.9339 - 2.9053 (t, J = 5.72 Hz, 2H), 2.8536 - 2.8527 (t, J = 5.58 Hz, 2H), 1.9357 - 1.9059 (t, J = 5.96 Hz, 2H), 1.2411 - 1.2058 (t, J = 7.06 Hz, 2H). ^{13}C NMR (100 MHz, DMSO-d_6): δ (*ppm*) 162.85, 158.83, 146.97, 132.12, 130.19, 129.18, 127.49, 125.45, 124.63, 122.46, 36.31, 28.88, 22.92, 14.41, 11.32. HR-MS (ESI): $[M]^+$ calcd for $C_{40}H_{37}N_2OS^+$ 593.2621, found, 593.2601.

Synthesis of TPA-2T-OS.

A mixture of TPA-2T (0.5 g, 1.14 mmol) and 6-(diethylamino)-1, 2, 3, 4-tetrahydroxanthylium (0.45 g, 1.25 mmol) in acetic anhydride (20 mL) were refluxed for 6 h. Then, the cooled mixture was concentrated in vacuum. The crude product was purified by column chromatography with DCM and methanol (v/v = 8:1) as an eluent. Finally, **TPA-2T-OS** (0.53 g, yield: 60.2 %) was obtained as green powders. ^{1}H NMR (400 MHz, DMSO-d_6) δ: 8.4077 - 8.3853 (*d*, J = 8.96 Hz, 1H), 8.2280 - 8.2060 (*d*, J = 8.8 Hz, 1H), 7.9126 (s, 1H), 7.8333 - 7.7765 (m, 1H), 7.6401 (s, 1H), 7.5273 - 7.4707 (m, 4H), 7.3699 - 7.2926 (m, 6H), 7.1507 (s, 1H), 7.0933 - 7.0225 (m, 6H), 6.9289 - 6.9073 (*d*, J = 8.8 Hz, 2H), 3.6594 - 3.6427 (*d*, J = 6.68 Hz, 4H), 2.6905 (s, 4H), 1.9149 (s, 2H), 1.2358 - 1.2010 (*t*, J = 6.96 Hz, 6H). ^{13}C NMR (100 MHz, DMSO-d_6): δ (*ppm*) 162.7946, 162.6075, 158.6915, 155.9757, 147.8326, 147.1627, 144.1627, 138.1337, 134.8326, 130.2878, 125.1303, 124.2969, 122.8865, 118.8530, 36.2540, 31.3418, 19.2690 HR-MS (ESI): $[M]^+$ calcd for $C_{44}H_{39}N_2OS_2^+$ 675.2498, found, 675.2473.

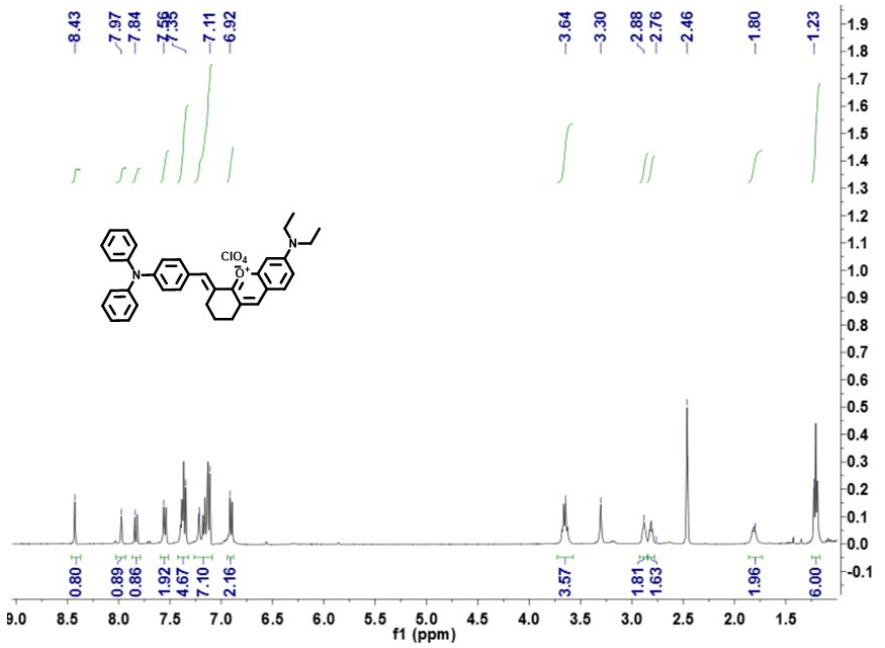

Figure S1. The 400 MHz ^{1}H NMR spectrum of **TPA-OS** in the DMSO-d_6 solution.

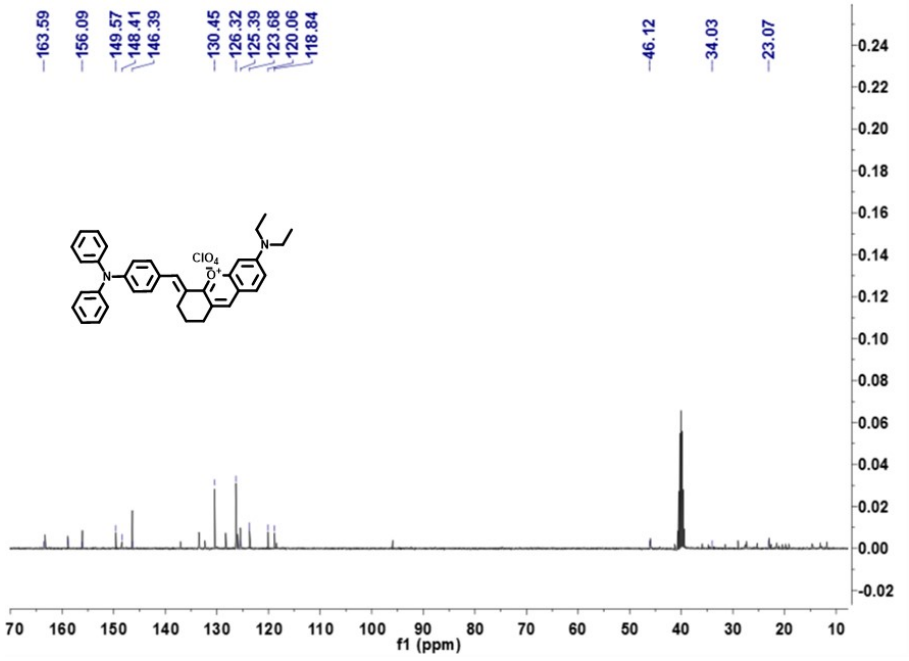

Figure S2. The 100 MHz ^{13}C NMR spectrum of **TPA-OS** in the DMSO-d_6 solution.

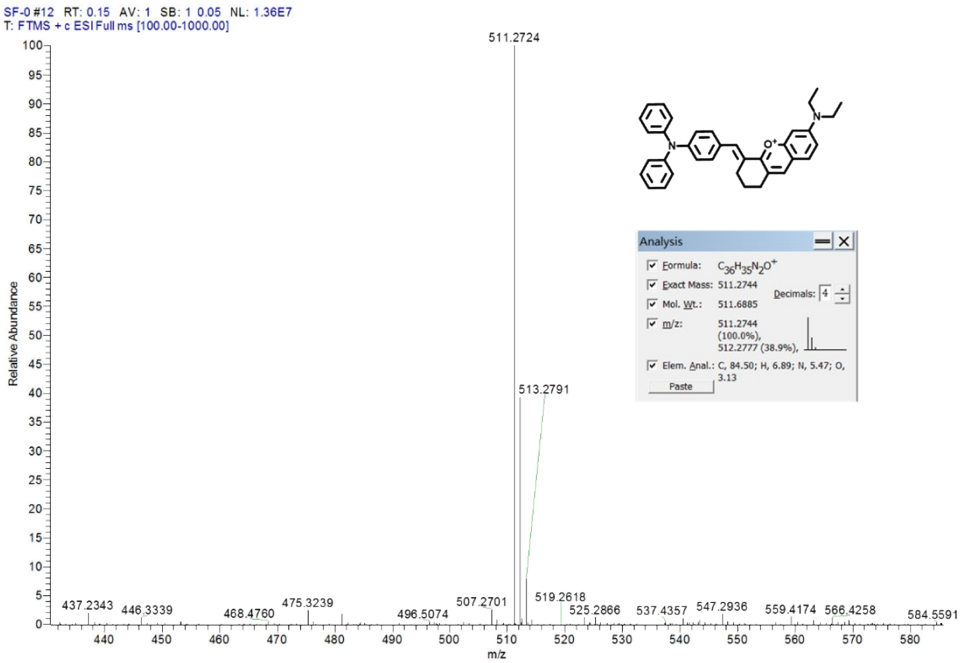

Figure S3. ESI-Mass spectrum of **TPA-OS** in methanol.

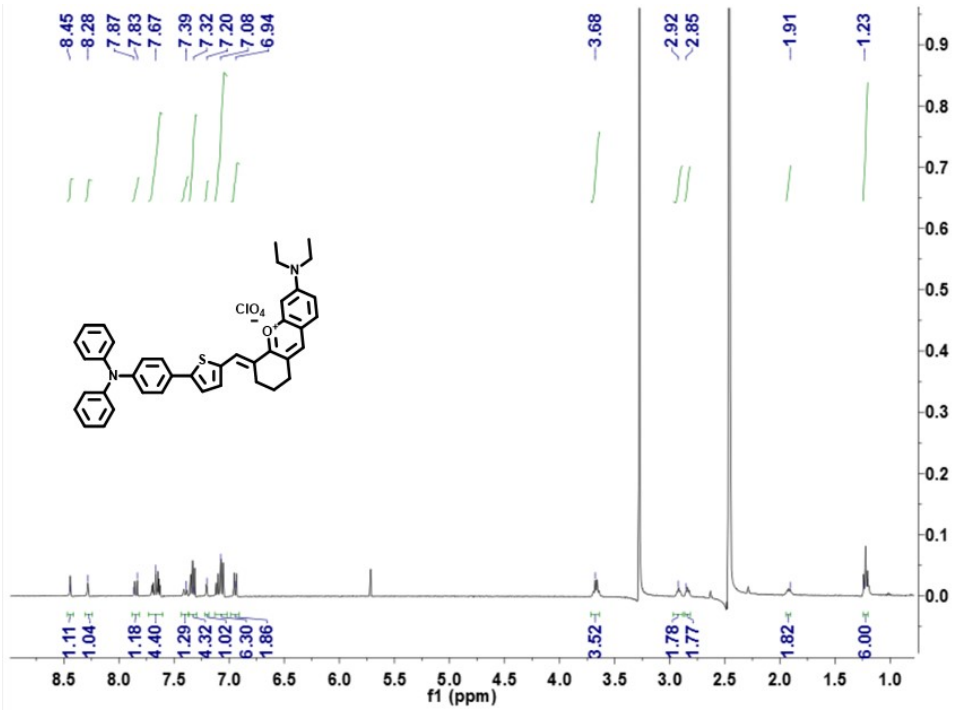

Figure S4. The 400 MHz ^{1}H NMR spectrum of **TPA-T-OS** in the DMSO-d_6 solution.

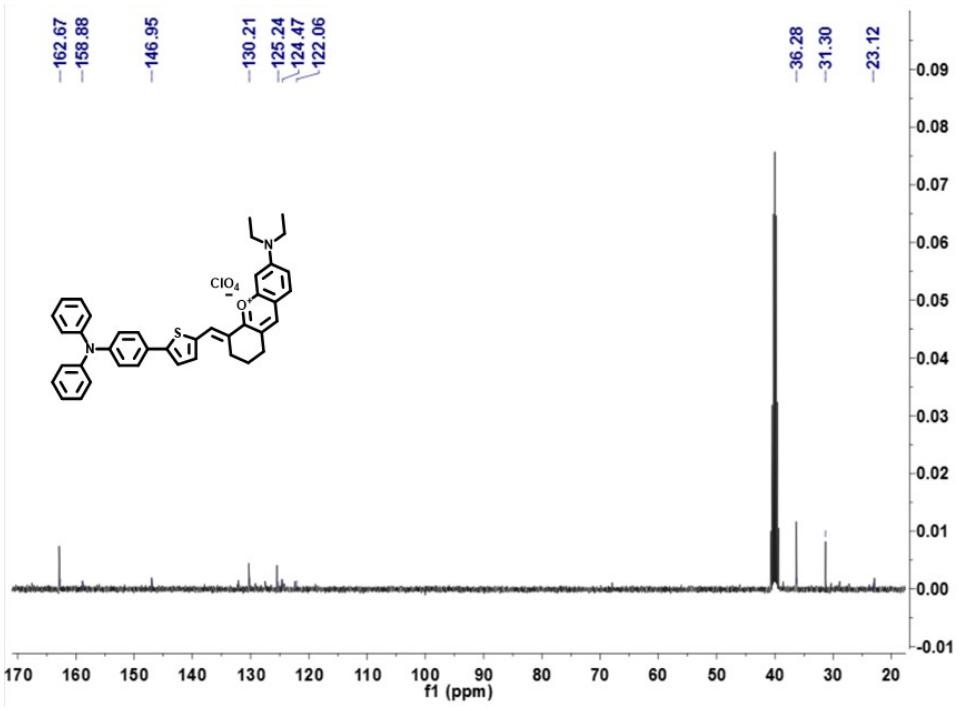

Figure S5. The 100 MHz ^{13}C NMR spectrum of **TPA-T-OS** in the DMSO-d_6 solution.

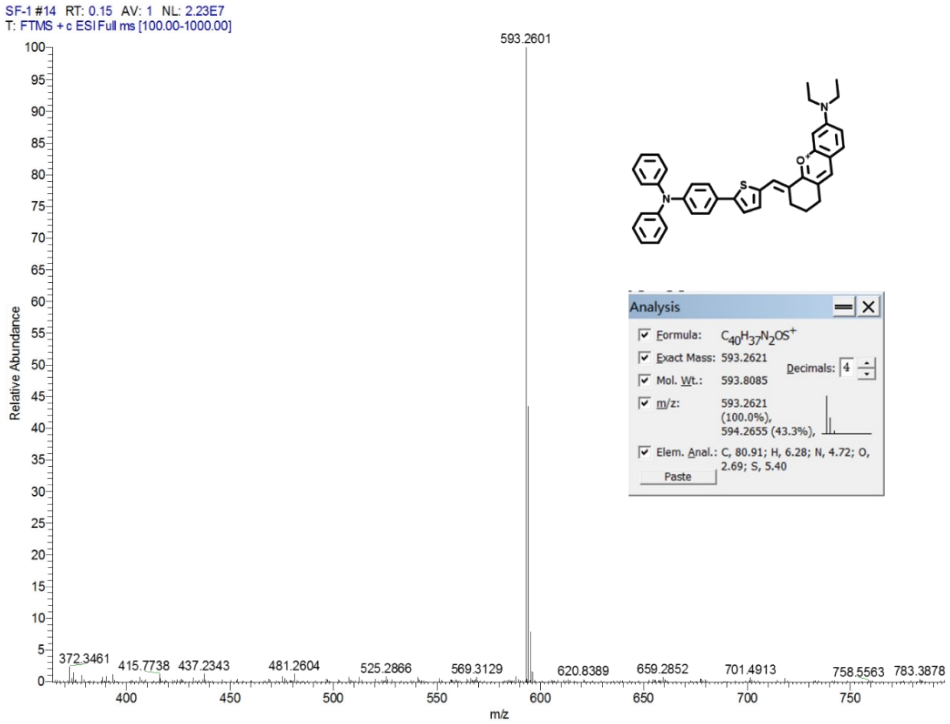

Figure S6. ESI-Mass spectrum of **TPA-T-OS** in methanol.

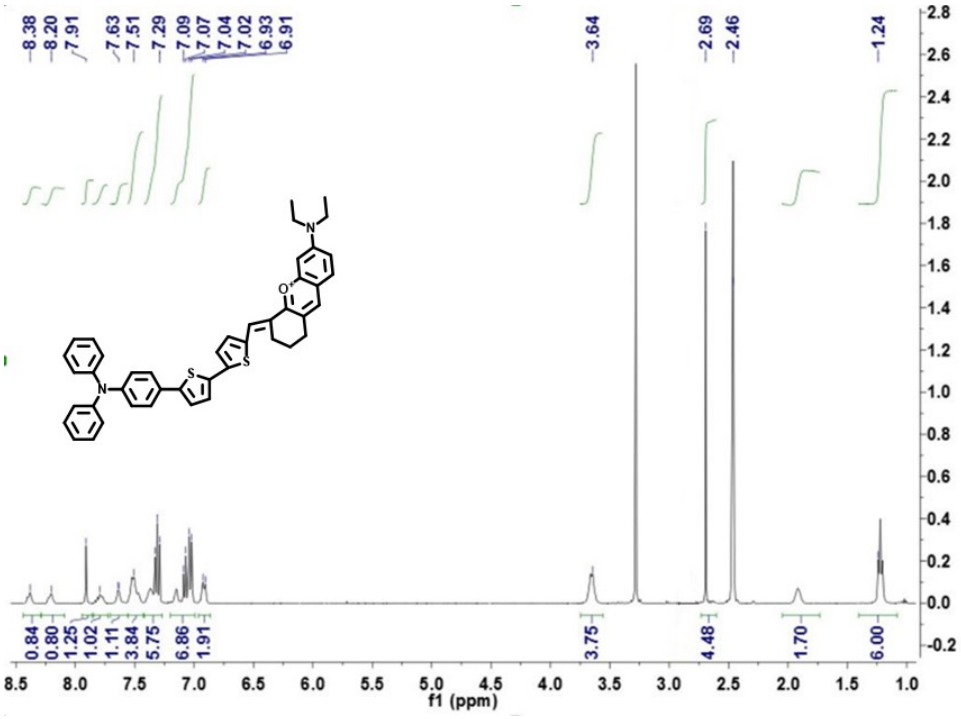

Figure S7. The 400 MHz ^{1}H NMR spectrum of **TPA-2T-OS** in the DMSO-d_6 solution.

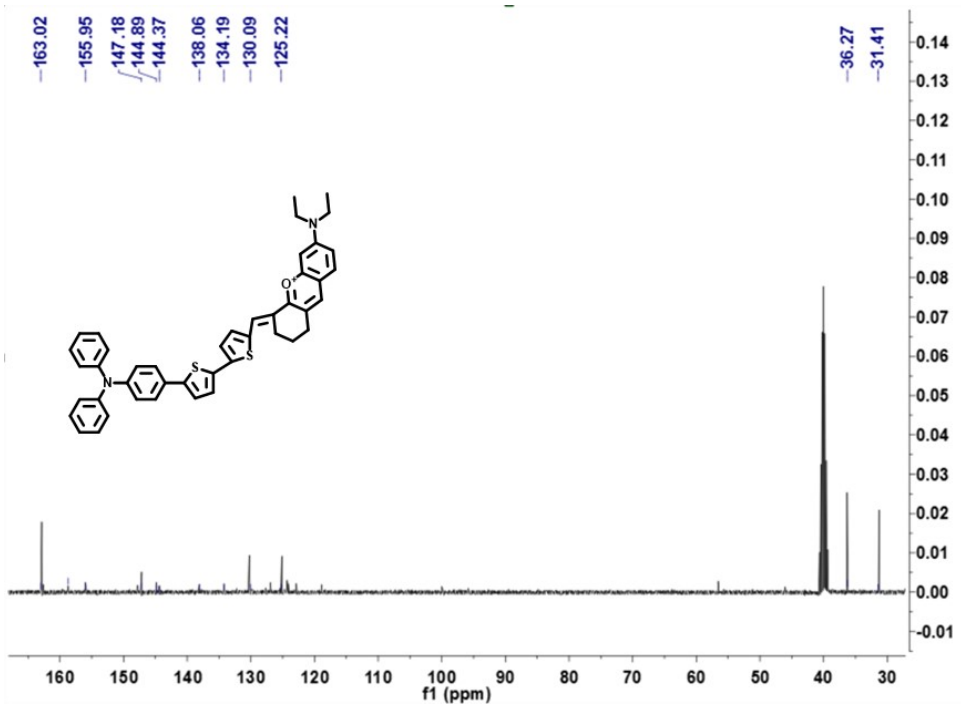

Figure S8. The 100 MHz ^{13}C NMR spectrum of **TPA-2T-OS** in the DMSO-d_6 solution.

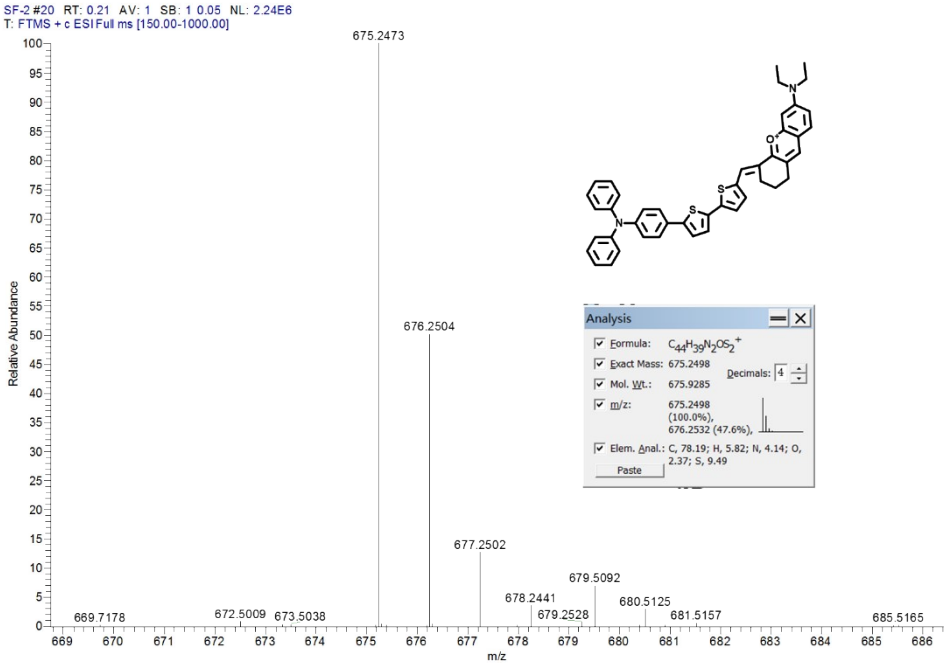

Figure S9. ESI-Mass spectrum of **TPA-2T-OS** in methanol.

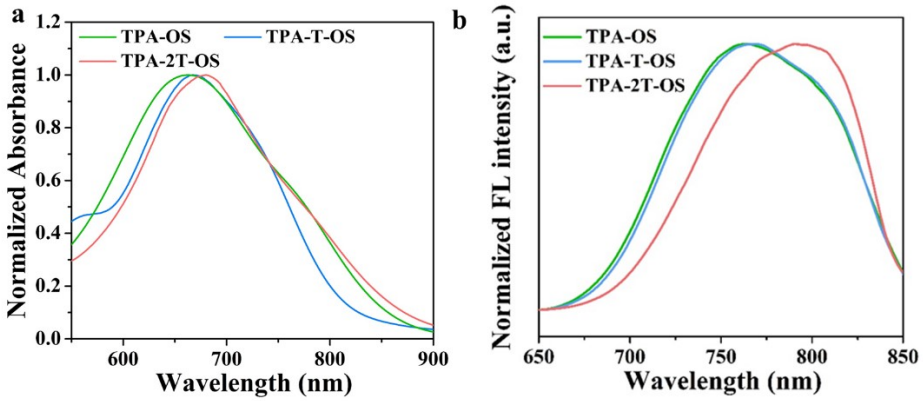

Figure S10. a) Normalized absorption spectra and b) normalized FL spectra of three AIE-PSs (1×10^{-5} M) in an aqueous solution.

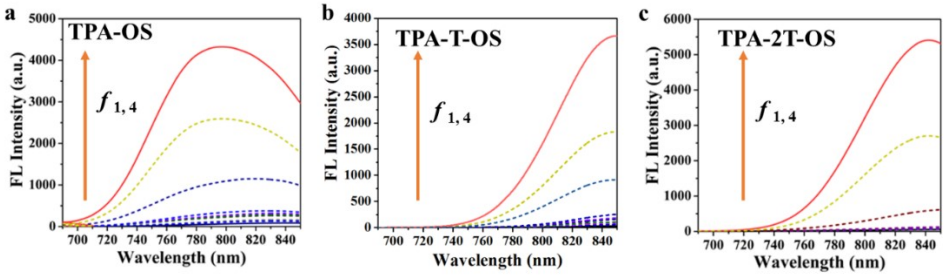

Figure S11. Plots of the FL intensity of three AIE-PSs versus DMSO and 1, 4 dioxane fraction.

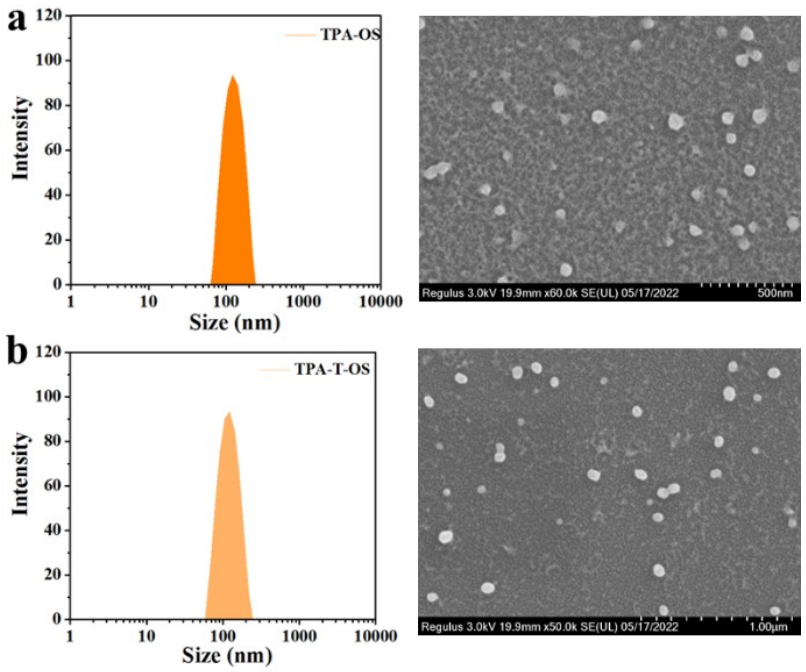

Figure S12. DLS and SEM images of a) **TPA-OS** and b) **TPA-T-OS** in H_2O.

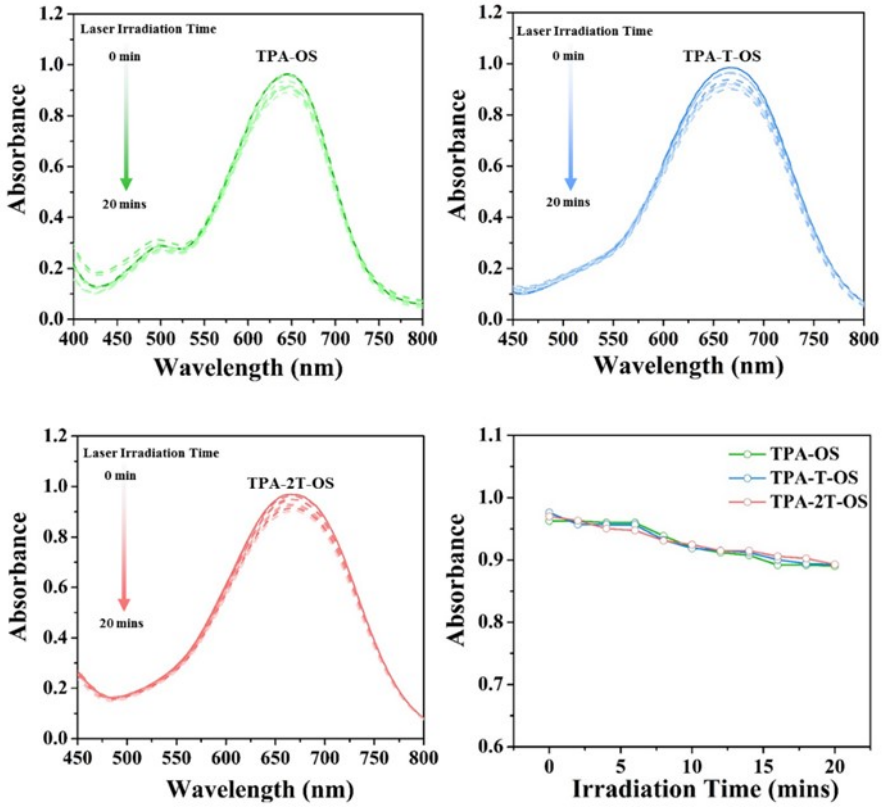

Figure S13. The photostability of three AIE-PSs.

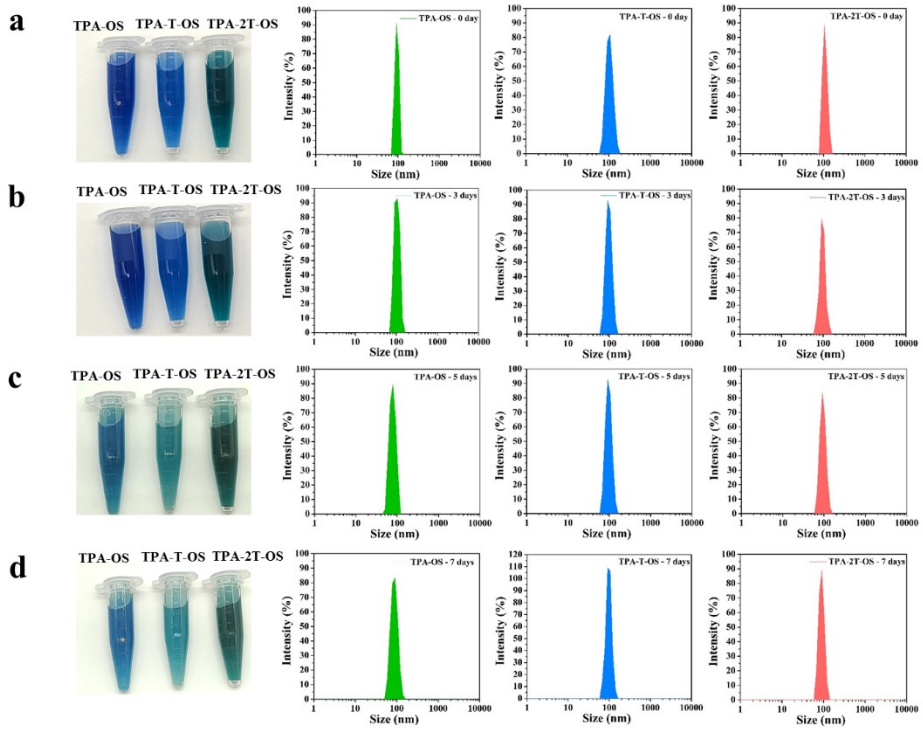

Figure S14. The water solubility test of AIE-PSs on a) Day 0, b) Day 3, c) Day 5 and d) Day 7.

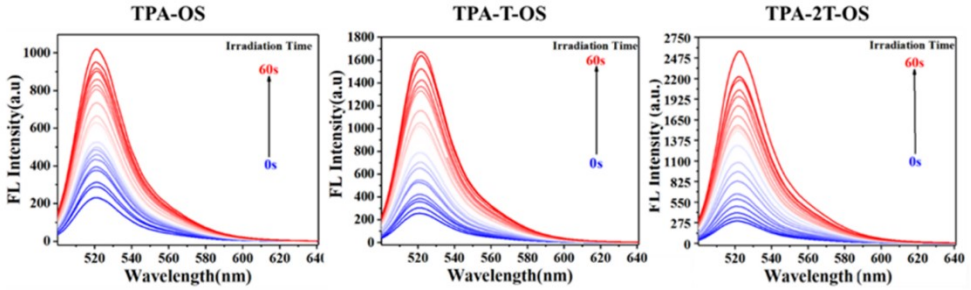

Figure S15. The fluorescence intensity of DCFH-DA (a fluorescence indicator of ROS) under laser irradiation (720 nm, 1 W cm^{-2}).

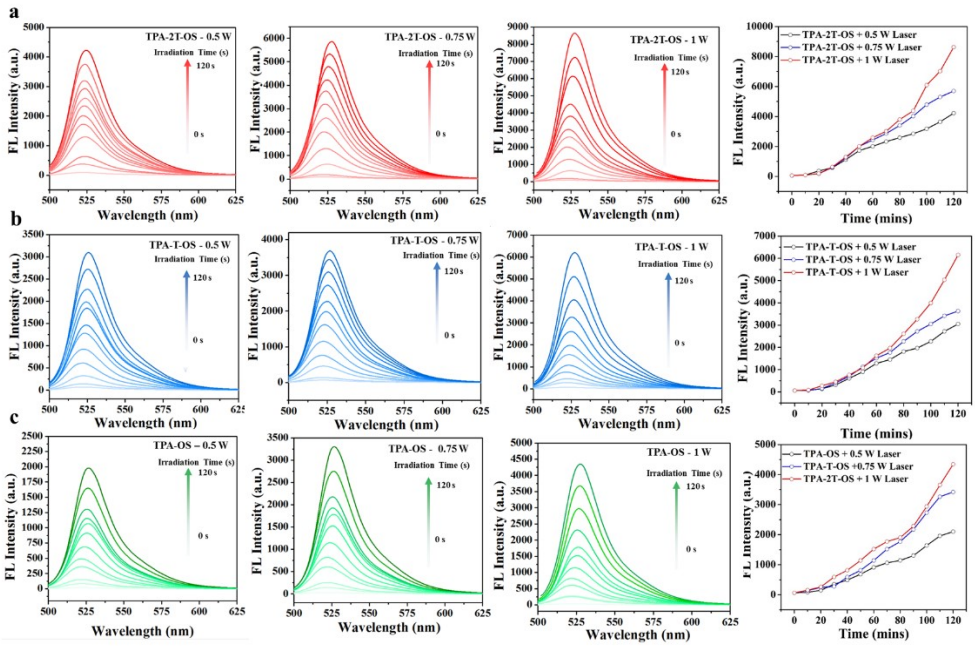

Figure S16. Comparison of the FL intensity at 530 nm of DCFH-DA with a) **TPA-2T-OS**, b) **TPA-T-OS** and c) **TPA-OS** upon different NIR-laser power (0.5 W cm^{-2}, 0.75 W cm^{-2}, and 1 W cm^{-2}) irradiation.

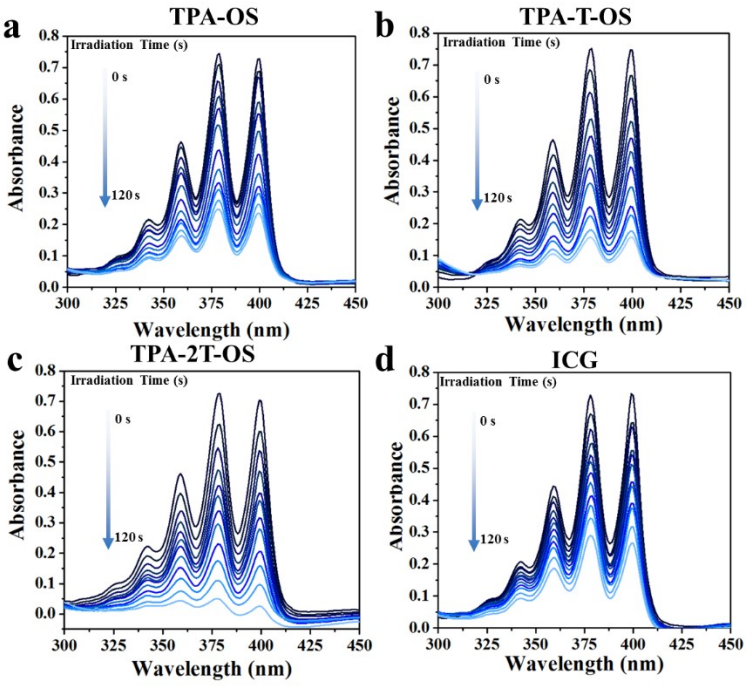

Figure S17. The absorbance of ABDA (an indicator of $^1O_2$) using under laser irradiation (720 nm).

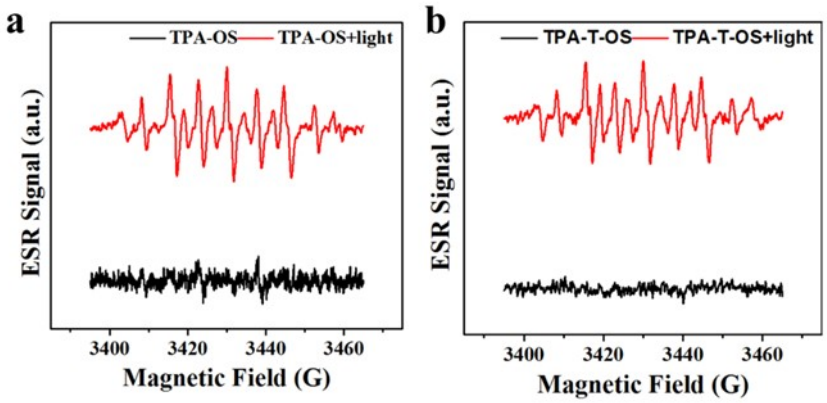

Figure S18. ESR spectra of DMPO/•OH for a) **TPA-OS** and b) **TPA-T-OS** in DMSO under irradiation for 1 minute.

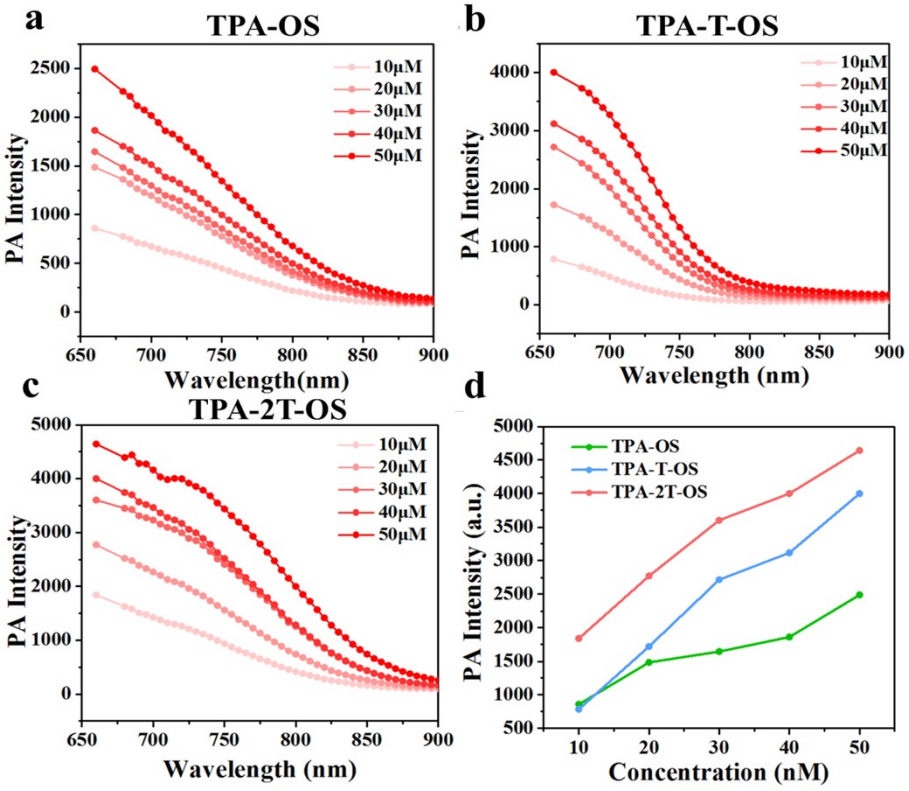

Figure S19. *In vitro* PA intensity of a) **TPA-OS**, b) **TPA-T-OS**, and c) **TPA-2T-OS** in different concentrations. d) The Photoacoustic intensity of three PSs at 660 nm under different concentrations and data were obtained from a), b), and c).

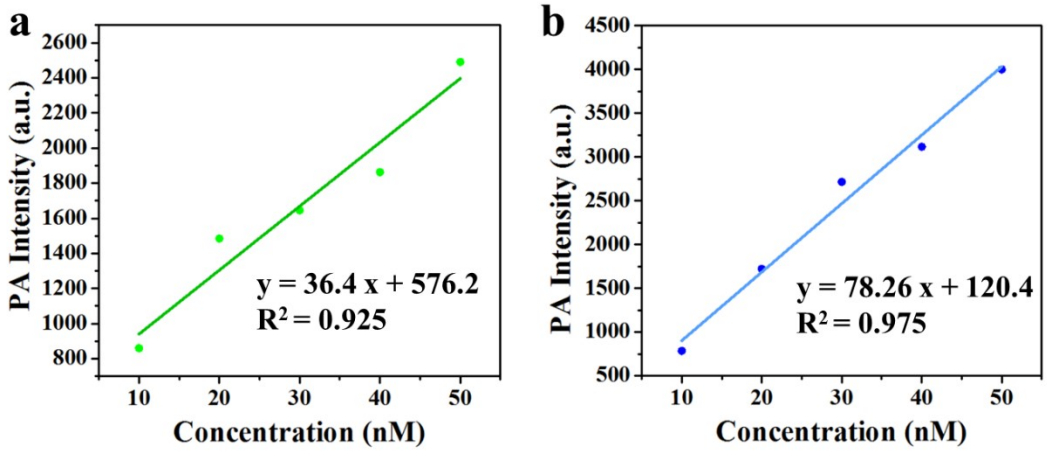

Figure S20. The linear relationship between the photoacoustic intensity of a) **TPA-OS** and b) **TPA-T-OS** and concentration.

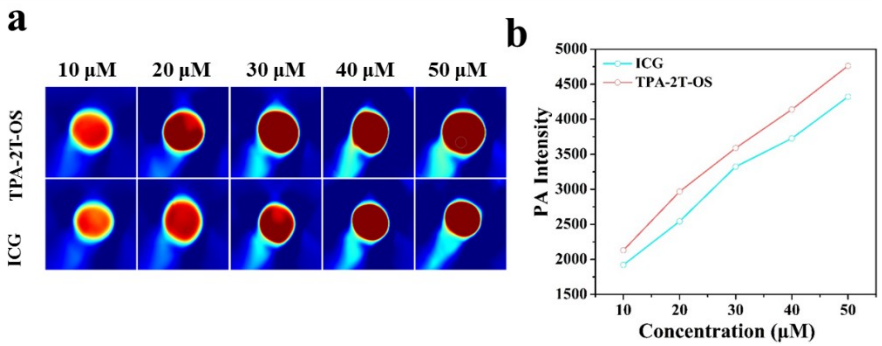

Figure S21. a) *In vitro* photoacoustic images of **TPA-2T-OS** and ICG. b) The Photoacoustic intensity of **TPA-2T-OS** and ICG under different concentrations.

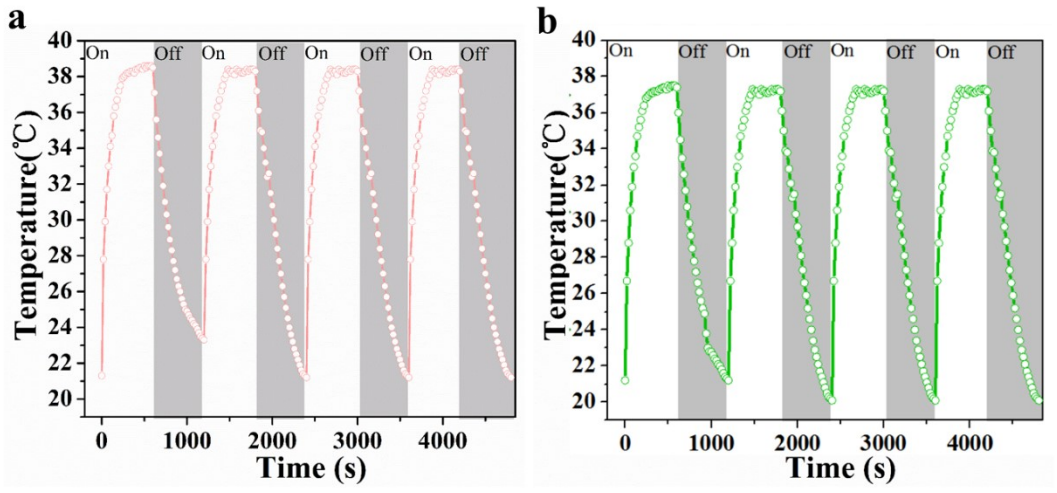

Figure S22. Photothermal stability of a) **TPA-OS** and b) **TPA-T-OS** under laser irradiation (720 nm, 1 W cm^{-2}) for four cycles.

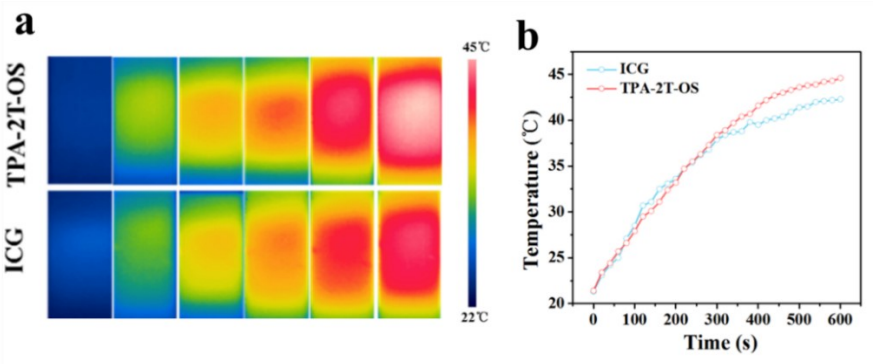

Figure S23. a) Infrared thermography of **TPA-2T-OS** and ICG within 10 min of laser irradiation. b) The relationship between photothermal intensity and time.

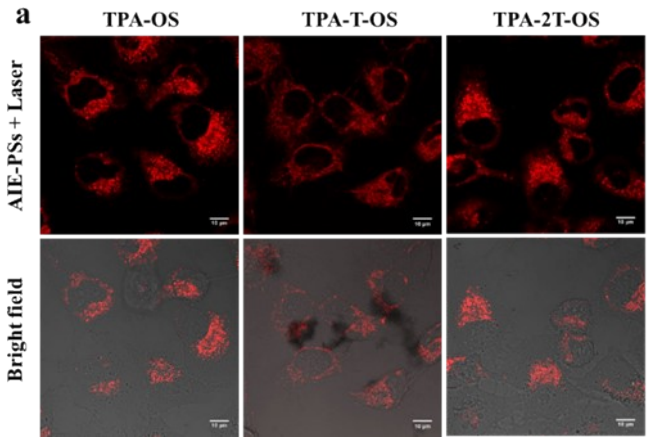

Figure S24. Confocal imaging of TPA-OS, TPA-T-OS, and TPA-2T-OS (10 μL, 1×10^{-5} mol L^{-1}) in HepG2 cells. Scale bar: 10 μm.

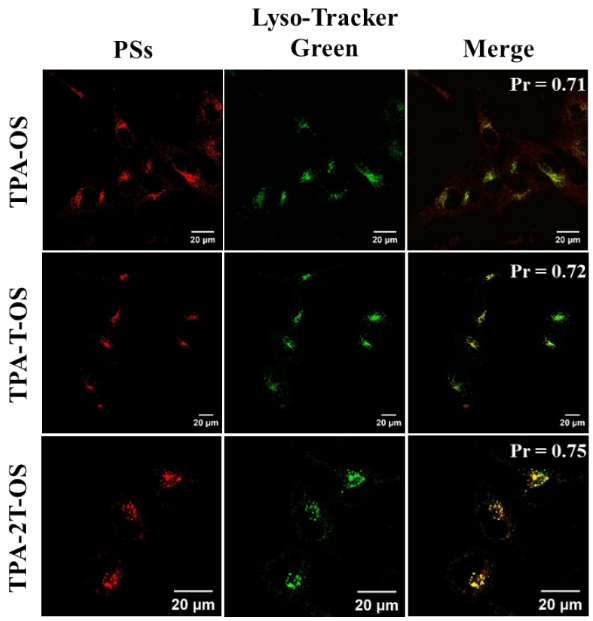

Figure S25. Colocalization experiment of HepG2 cells treated with 10 μL (1×10^{-5} mol L^{-1}) of AIE-PSs and 1 μL of Lyso-Tracker in 1 mL PBS.

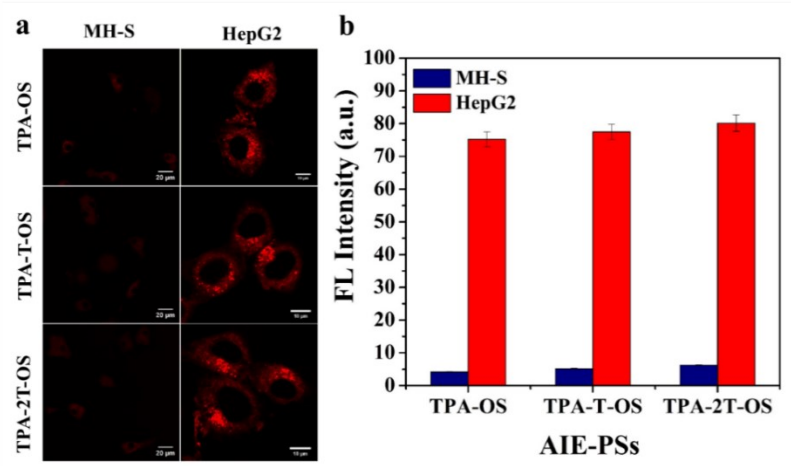

Figure S26. a) Confocal imaging of three AIE-PSs in HepG2 cells and MH-S cells and b) comparison of their fluorescence intensity in cells.

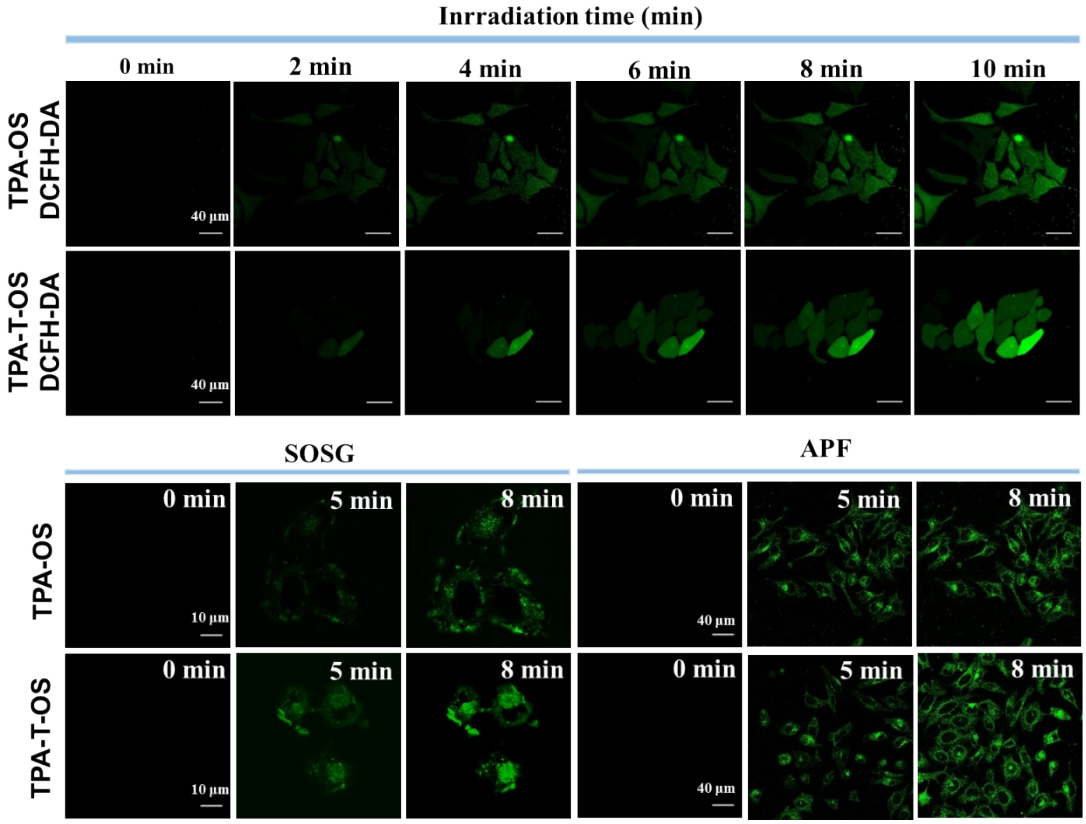

Figure S27. Confocal laser scanning microscopy images of HepG2 cells treated under different conditions and stained with DCFH-DA, SOSG, and APF.

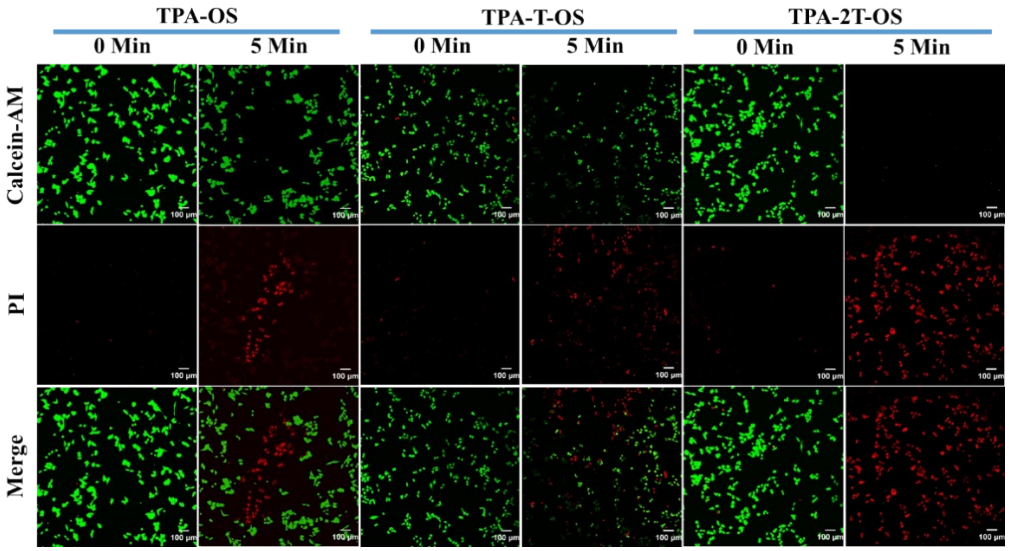

Figure S28. Calcein-AM/PI-Live/dead assay of HepG2 cells.

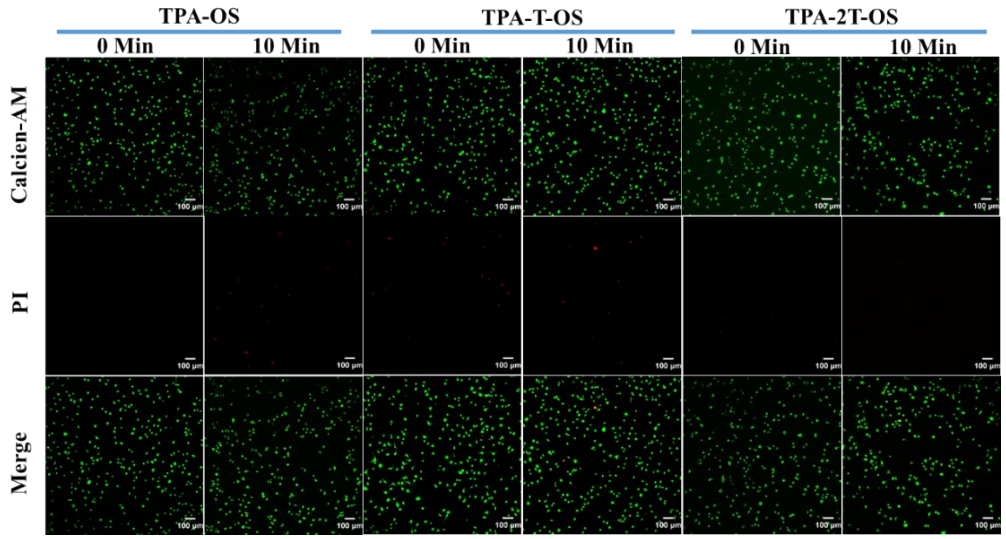

Figure S29. Calcein-AM/PI-Live/dead assay of MH-S cells.

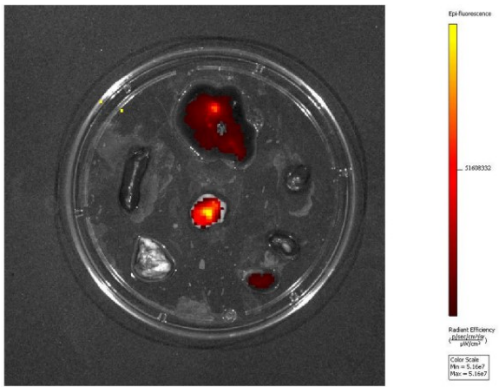

Figure S30. Fluorescence images of the dissected tissues and tumors 4 h after the injection of **TPA-2T-OS.**

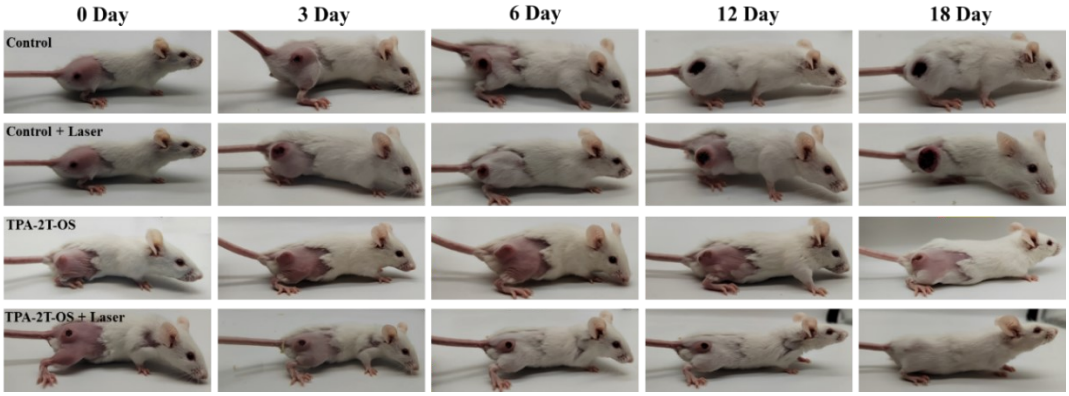

Figure S31. Photographs of tumor *in vivo* under different treatments during 18 days of observation, control: mice without injection of **TPA-2T-OS** under different treatments time with laser.

Table 1. Crystal data and structure refinement for the **TPA-OS** nanocluster. CCDC number is 2177259.

Crystal system	monoclinic
Space group	P 1 21/c 1
a/Å	10.1361(4)
b/Å	20.8271(8)
c/Å	15.0291(5)
α/°	90
β/°	97.033(3)
γ/°	90
Volume/Å^3	3148.9(2)
Z	4
ρcalcg/cm^3	1.289
μ/mm^{-1}	1.444
F(000)	1288.0
Radiation	CuKα (λ = 1.54186)
Index ranges	-6 ≤ h ≤ 18, -64 ≤ k ≤ 59, -21 ≤ l ≤ 20
Final R indexes [I>=2σ (I)]	R1 = 0.0498, wR2 = 0.1524
Final R indexes [all data]	R1 = 0.0816, wR2 = 0.2095

Table 2. Crystal data and structure refinement for the **TPA-T-OS** nanocluster. CCDC number is 2177143.

Crystal system	monoclinic
Space group	P -1
a/Å	9.2481(9)
b/Å	10.6765(11)
c/Å	20.117(2)

α/°	86.255(8)
β/°	85.743(8)
γ/°	67.366(8)
Volume/Å^3	1826.8(3)
Z	2
ρcalcg/cm^3	1.415
μ/mm^{-1}	3.204
F(000)	812
Radiation	CuKα (λ = 1.54186)
Index ranges	-6 ≤ h ≤ 18, -64 ≤ k ≤ 59, -21 ≤ l ≤ 20
Final R indexes [I>=2σ (I)]	R1 = 0.0706, wR2 = 0.2179
Final R indexes [all data]	R1 = 0.0816, wR2 = 0.2095

Table 3. Crystal data and structure refinement for the **TPA-2T-OS** nanocluster. CCDC number is 2177142.

Crystal system	monoclinic
Space group	P -1
a/Å	9.1378(13)
b/Å	10.9014(16)
c/Å	22.637(3)
α/°	97.152(11)
β/°	97.379(11)
γ/°	113.666(11)
Volume/Å^3	2009.4(5)
Z	2
ρcalcg/cm^3	1.281
μ/mm^{-1}	2.192
F(000)	811.3
Radiation	CuKα (λ = 1.54186)
Index ranges	-6 ≤ h ≤ 18, -64 ≤ k ≤ 59, -21 ≤ l ≤ 20
Final R indexes [I>=2σ (I)]	R1 = 0.0800, wR2 = 0.2699
Final R indexes [all data]	R1 = 0.0816, wR2 = 0.2095

REFERENCE

[1] S. Wang, M. Rong, H. Li, T. Xu, Y. Bu, L. Chen, X. Chen, Z.P. Yu, X. Zhu, Z. Lu, H. Zhou, Unveiling Mechanism of Organic Photogenerator for Hydroxyl Radicals Generation by Molecular Modulation, *Small* 18(6) (2022) e2104857.